ANALYTICAL THERMAL MODEL OF A GENERIC MULTI-LAYER SPACERLESS 3D PACKAGE

by

ERANTHA NUWAN RODRIGO

Presented to the Faculty of the Graduate School of

The University of Texas at Arlington in Partial Fulfillment

of the Requirements

for the Degree of

MASTER OF SCIENCE IN MECHANICAL ENGINEERING

THE UNIVERSITY OF TEXAS AT ARLINGTON

August 2008

ACKNOWLEDGEMENTS

I would like to thank Dr. Dereje Agonafer for giving me the opportunity to work at the EMNSPC and conduct research. His guidance, knowledge and encouragement have helped in all aspects of this project. I would also like to express my appreciation to Dr. A. Haji-Sheikh and Dr. S. Nomura for taking tome to be on my review committee and guiding me through this project.

I would also like to thank all the members of EMNSPC for their support and willingness to be of assistance at all times.

June 20, 2008

ABSTRACT

ANALYTICAL THERMAL MODEL OF A GENERIC MULTI-LAYER SPACERLESS 3D PACKAGE

ERANTHA NUWAN RODRIGO, M.S.

The University of Texas at Arlington, 2008

Supervising Professor: Dereje Agonafer

The need for more functions in a single device has lead to die stacking architecture. Although the number of die increases further to accommodate package functionality, the overall package dimensions have not increased, they have stayed the same or decreased (roughly 1.4mm). Recently, Samsung announced a 16 dice stacked device. If this trend continues, in order to keep the same package height, alternate stacking structures need to be investigated. One such opportunity is spacerless die stacking architecture. Using dummy silicon spacers add cost to a package and do not increase the memory or functionality although the spacers serve as enablers for wire bonding of same size dice. Spacerless architecture reduces the package height by eliminating spacers or dummy dice. This allows for an increased number if active die to

be stacked directly on one another without changing the overall package height, or in some cases reducing the package height.

Previous work (Haji-Sheikh et al) has been done to develop steady-State heat conduction model in a two-layer body. This analytical model will be extended to the current multi-layered generic spacerless three dimensional packages (3DP) enabling the computation of temperature for uniform powered dice. The computation will account for the contact resistance created by the die attach and the solder balls. The aim is to formulate an analytical method to calculate the temperature on an increased number of dice without reformulating equations for each configuration.

TABLE OF CONTENTS

Appendix

LIST OF ILLUSTRATIONS

LIST OF TABLES

CHAPTER 1

INTRODUCTION

1.1 3D Package

The 3D Package is a relatively new development in packaging technology emerging within the last 15 years. The 3D package consists of dice being stacked on top of each other in various configurations in order to include an increased number of functional dice in a single package with a small footprint. Stacking can greatly increase the functionality of a package while simultaneously reducing the foot print of the overall package leading to considerably smaller electronic devices. Stacking dice is a powerful way of maximizing the functionality and performance per unit area if the package footprint reducing the overall size of the package. Initially 3D packages were limited to two layers, with the increased functionality requirements packages have evolved to have a larger number of dice in a single package. Recently Samsung announced the development of a 3D package including 16 dice. Since the advent of 3D architecture being implemented in the mid 90's the number of 3D packages incorporating flash memory and SRAM had grown to 60 million units in the year 2000, [11] since then it has been increasing at a rate of 50% each year.

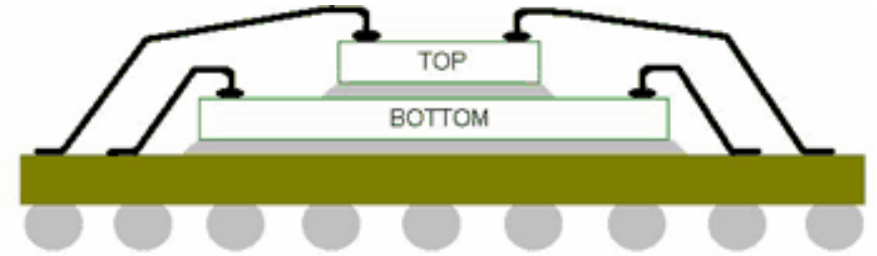

Figure 1.1: Pyramid Type 3D Package

3D packages are built in many different types of architectures. So me of the most common types of 3D packages are staggered die 3D packages, rotated, pyramid and spacer type 3D packages. In each case it is vital to have the physical space to attach interconnects to each die. Each architecture has been designed with surface area to facilitate interconnects. All of these architectures lose functional die space to facilitate interconnects.

Pyramid type packages lose functional die space by reducing each subsequent die size to create a surface for interconnects, staggered packages use are designed to have over hang to accommodate interconnects. Overhang can cause structural reliability concerns. Spacer type packages use dummy dice as spacers and increase the height and cost of the overall package. Figure [1.2] shows these three types of architecture. [14]

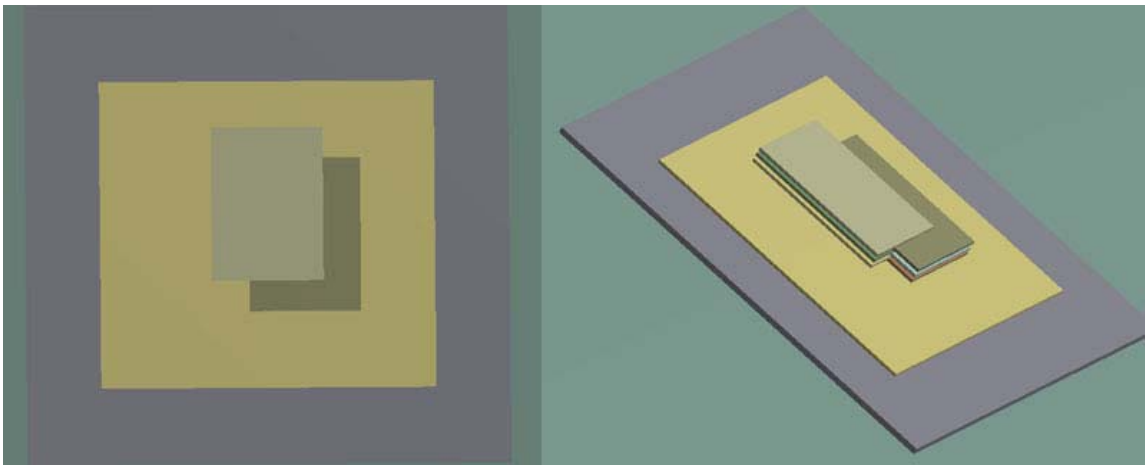

Figure 1.2: Staggered Stack 3D Package

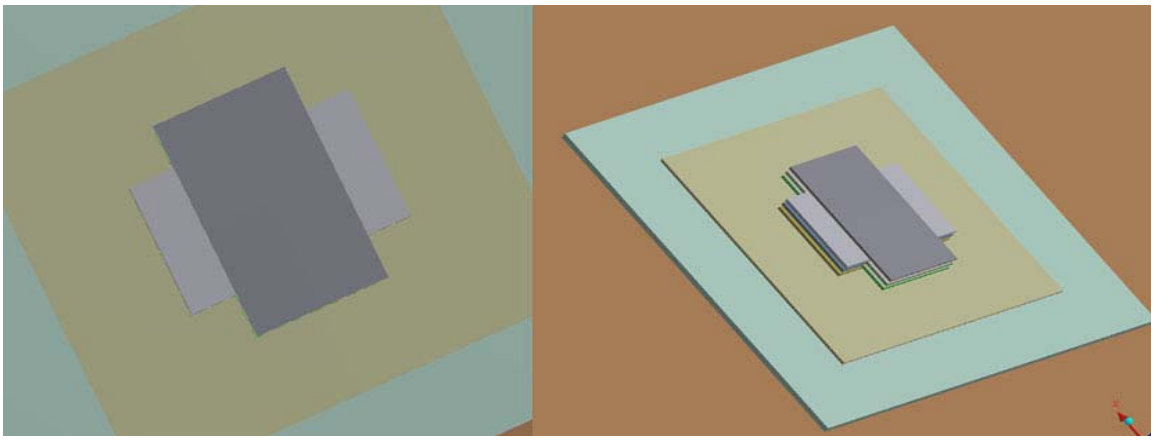

Figure 1.3: Rotated Stack 3D Package

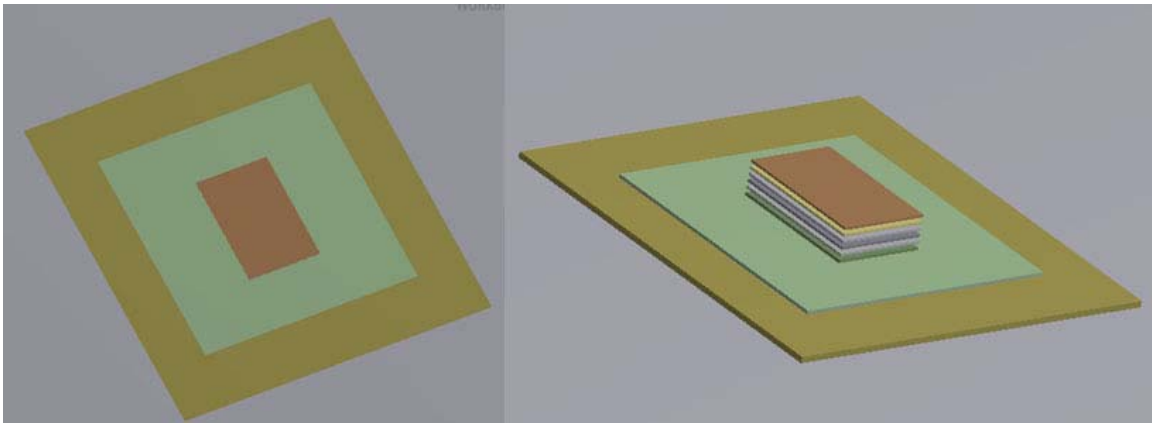

Figure 1.4: Spacer-Die Stack 3D Package

As 3D packaging technology is used in a large number of applications such as cell phones, PDA's, and mobile computing, 3D packaging technology advancements have allowed for an increase number of functional dice to be packaged in a smaller package. One such technology is spacerless 3D packaging.

1.1.1 Evolution of 3D packages

3D packages were first used in memory applications where space limitations were a constraint. In devices such as cell phones the trend is to reduce the overall size while increasing the number of functions incorporated in the package. One of the earliest applications is cell phone manufacturers used 3D architecture to integrate flash memory and static read access memory (SRAM) into a single chip. With the trend of wireless devices becoming smaller in size while simultaneously incorporating an increased number of functions such as phones, organizers and cameras, 3D package

technology has advanced a great deal to keep up with this demand. The following illustration shows the roadmap for 3D packaging as presented by Intel.

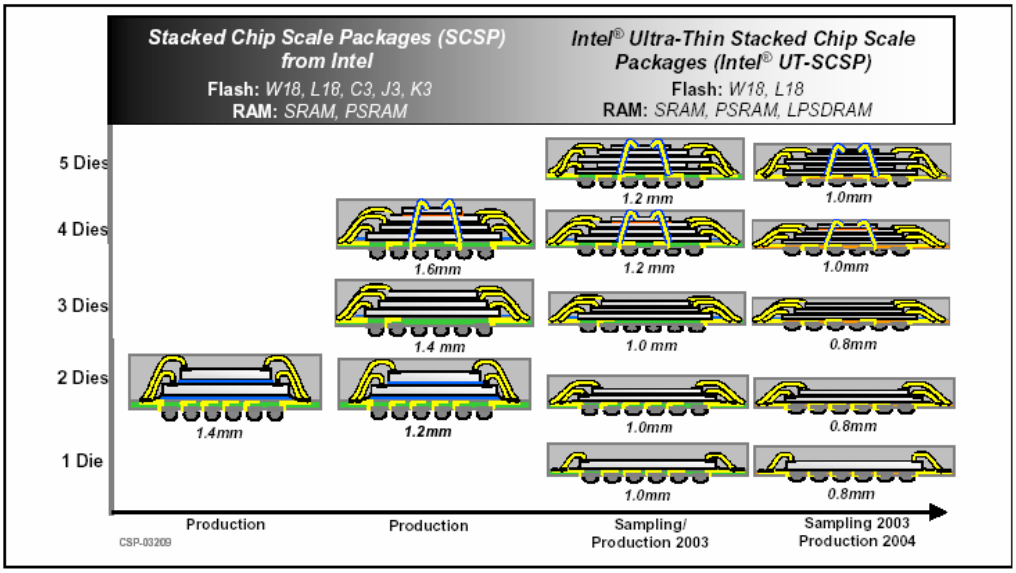

Figure 1.5: Intel Roadmap for 3D Packaging.

In order to accommodate the increased number of functions electronic devices are including a larger number of dice in a single stack. As the number of dice have increased in a single stack the total package height does not increase accordingly to accommodate the additional dice in the package. The overall package height stays the same, or in many cases is reduced as the number of functional dice is increased. Traditionally a standard package height has been 1.4 mm for stacked die packages. As demand for smaller packages increase the height is being reduced to 1.2 mm and 1.0 mm packages as well as 0.8 mm packages in some cases. This overall package height includes the substrate, die, spacers and BGA height. This trend is illustrated in figure 1.6 by ChipPak Inc.

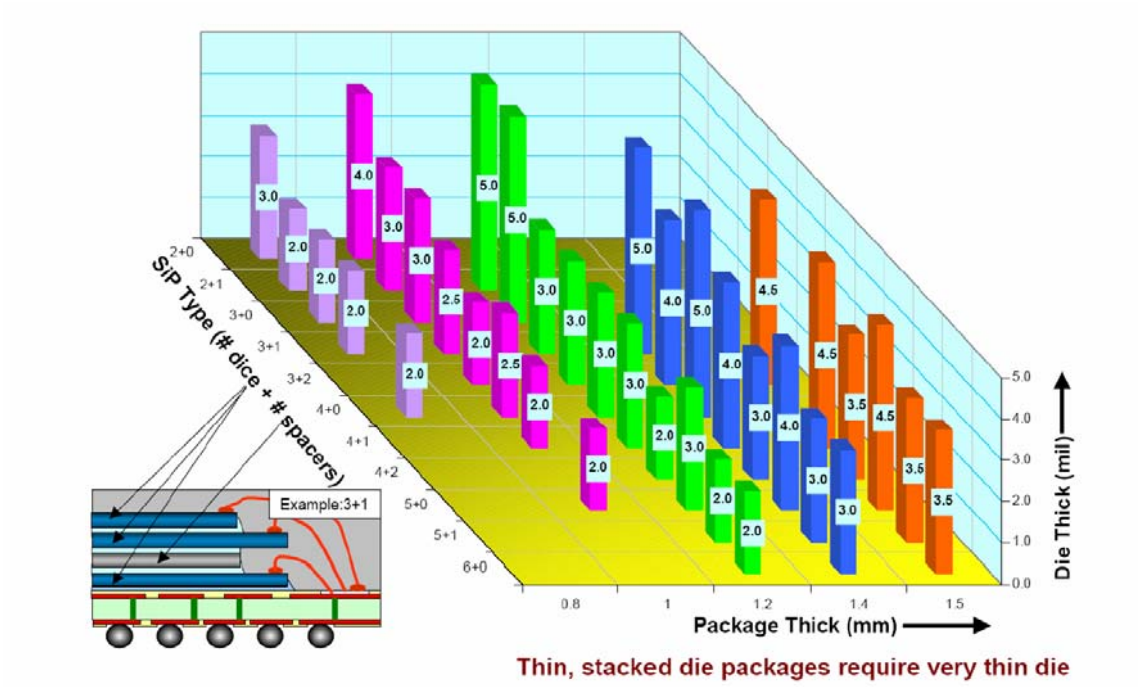

Figure 1.6: Trend in Package Height for 3D packages by ChipPak Inc.

In order to incorporate several functional dice in a single package with the size limitation requirements a variety of 3D package architectures have been developed. Some of these are, package on a package architecture, and system on a package architecture. Both of these technologies are designed to integrate several packages that traditionally have been packaged individually and mounted onto a printed circuit board. System in Package contains multiple packages such as flip chip ball grid array packages integrated on to one package. This technology allows for a several active and passive components such as processors and memory to be packages close to one another. Interconnect lengths are reduced and smaller package sizes are realized with this architecture.

System on a package architecture incorporates multiple packaged at the wafer level. Each functional device is incorporated into a single die structure. The stacked die architectures are most commonly used in this type of package. As shown in figure 1.67the three traditional types of stacked die architectures can be improved with better interconnect technologies.

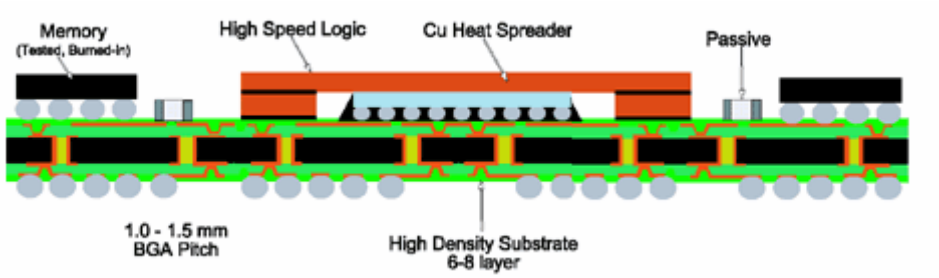

Figure 1.7: System on a package as presented by Amcor.

Interconnect technology has played a major role in the advancement of 3D packages. Technology such as through-silicon via has facilitated the stacking of dice with the same footprint without rotating or staggering any of the dice or including spacers. [10, 12]

1.1.2 Spacerless 3D packages

With package height reducing and the number if dice in a single package looking to be increased, spacerless 3D packages have several advantages. Removing spacers form a 3D package reduces the package height and there is no space used up by non functional dice. With the emergence of technologies such as through silicon vias,

packaging same size dice without spacers is possible. Figure shows an illustration of a spacerless 3D package.

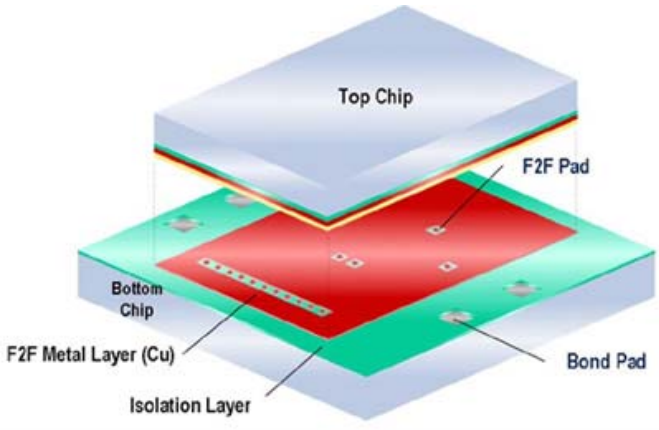

Figure 1.8: Spacerless Die Stack Package

Through silicon vias have been successfully used to create interconnects between a larger number of dice. Lee details a proposed spacerless package [11] and evaluates the thermal performance using a numerical simulation. Figure 1.9 and figure 1.10how the proposed package using through silicon vias and no spacers. Each package has interconnects through solder balls placer around the periphery of the package.

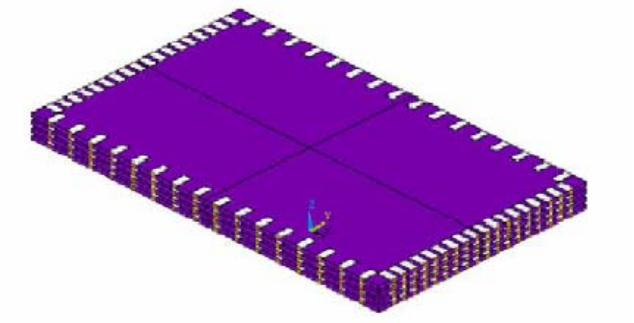

Figure 1.9: Spacerless 3D Package Model [11]

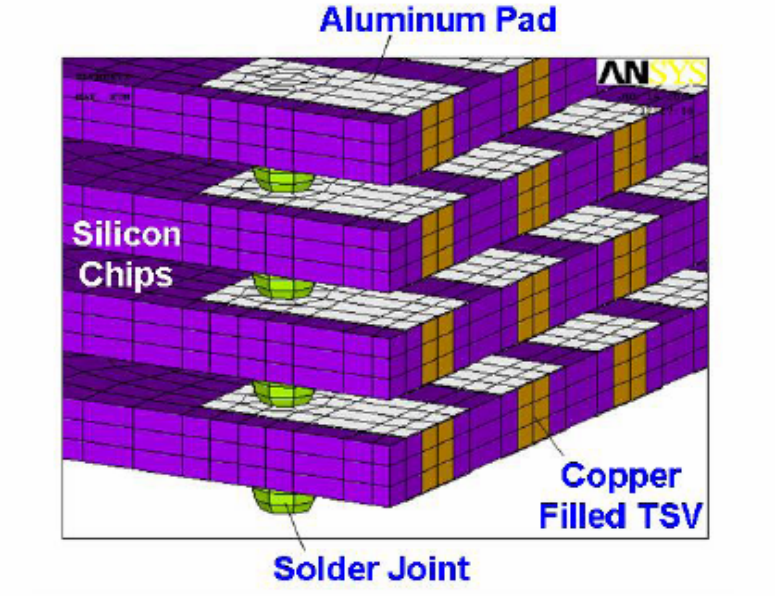

Figure 1.10: Spacerless 3D Package Model with Through Silicon Via Interconnects. [11]

1.2 Thermal Considerations of 3D Packages

When considering multilayered stacked die architecture one of the major concerns is accurately predicting the heat distribution. Knowing the heat distribution aids in identifying and eliminate hot spots and resulting failure. One of the reasons it is increasingly difficult to experimentally test multi layered die architecture is the higher probability of failure. If one single die fails in a multilayered structure, all the dice in the package are lost. This is a costly and inefficient method of testing architecture of this type. From this standpoint it is important to be able to numerically and analytically test such new die architecture. [1]

The thermal resistance of a package is used to characterize the heat flow between the package and the surroundings. The thermal resistance is calculated using equation 1.1 where θ_{JA} is the thermal resistance measured in degrees C/watt, between the junction temperature and the ambient, T_J is the junction temperature, T_∞ is the ambient temperature, and P is the power dissipation of the package in watts.

$$\theta_{JA} = (T_j - T_\infty) / P \tag{1.1}$$

In order for this method to be used it has been generally assumed the power in a package to be uniform. In the case of 3D packages with non uniform power distributions the spreading resistances and constriction resistances have a significant effect on the resulting junction temperature. An accurate junction temperature is important in order to predict the reliability of the package.

With the architecture of packages increasing in complexity the power distribution is increasingly nonlinear. Non linear power distributions cause hot spots on a package with significantly higher junction temperatures as compared to the same package being considered having a uniform power distribution with the same total power output. The architecture of a 3D package subsequently causes all of the surrounding dice to be subject to the non uniform temperature concentration. With the increased number of die being stacked an analytical model with the ability to accommodate an increasing number of dice will be greatly beneficial.

CHAPTER 2

LITERATURE REVIEW

2.1 Thermal Prediction of 3D Packages

Thermal prediction of 3D packages can be done using an analytical approach or a numerical approach. Using commercial software such as ANSYS, a numerical model can be constructed and solved to obtain a temperature solution. In this study the objective is to develop an analytical model for a spacerless 3D package.

2.1.1. Numerical Modeling of 3D Packages

As shown by Houssian, [6] a numerical simulation can be developed for various types of 3D packages. The solutions to the packages in figure 2.1 are detailed below. Each package is taken to have four functional dice with the bottom die having a 0.4 watt capacity and all others 0.3watts. The convection coefficient (h) is set at 5 W/m^2-^0C. The results are given in Table [2.1] and figure [2.1].

Table 2.1: Numerical Temperature Solutions. [6]

	Staggered Stack	**Rotated Stack**	**Spacer-Die Stack**
Maximum Temperature (^oC)	99.699	100.25	100.3

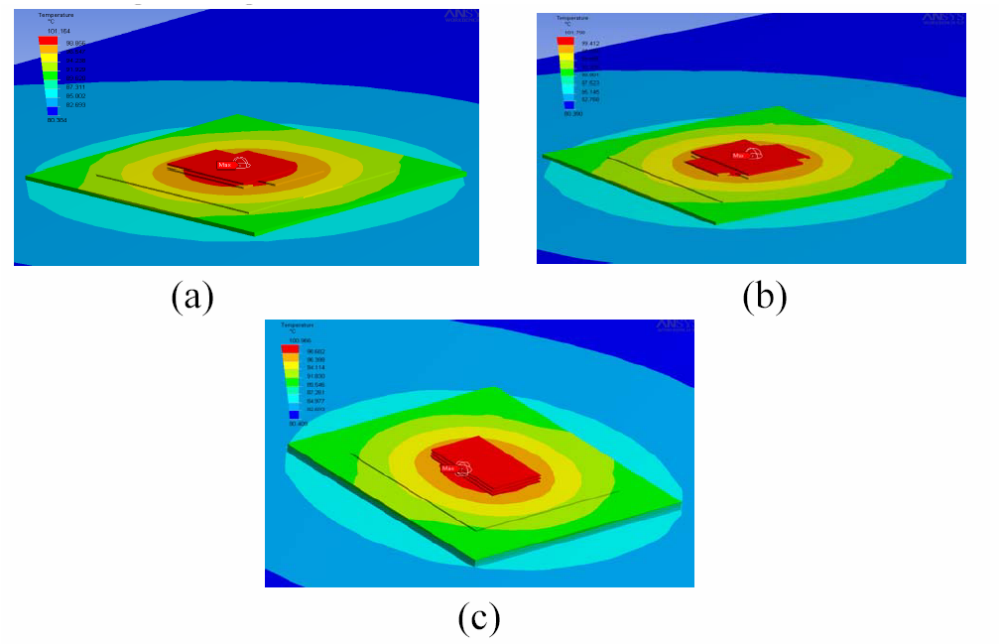

Figure 2.1: Solutions to Numerical Simulation: (a) Staggered Architecture, (b) Rotated Architecture, (c) Spacer Die-Stack Architecture [6]

2.2. Analytical Modeling of 3D package

2.2.1. Analytical Modeling of Heat Conduction in Steady State

Multidimensional steady state heat conduction problems are solved using the separation of variables method when one boundary condition is non nonhomogeneous. If more than one boundary conditions is non homogeneous, the problems can be broken in to several smaller problems each with one nonhomogeneous boundary condition. Solving each individual problem and using the separation of variables a solution can be obtained for the original problem. As detailed by Özişik [14] the following problem has more than one nonhomogeneous boundary condition. The diffusion equation (2.1) and the applied boundary condition (2.2) are as follows.

$$\nabla^2 T(\vec{r}) = 0 \tag{2.1}$$

$$k_i \frac{\partial T}{\partial n_i} + h_i T = f_i \tag{2.2}$$

Equation (2.2) shows more than one nonhomogeneous boundary condition being applied. $\delta/\delta n_i$ is the derivative along the outward normal direction of the surface S_i where the boundary condition is applied. i = 1,2,…,s, with s being the number of continuous boundary surfaces. f_i is the non homogeneous portion of the boundary condition at S_i. The problem is broken in to sections with one nonhomogeneous boundary condition for the temperatures represented by $T_j(\mathbf{r})$ as follows, i and j are indices equal to 1,2,…,s. δ_{ij} is the kronercker delta, for i≠j kronercker delta is equal to zero and for i=j kronercker delta is equal to one.

$$\nabla^2 T_j(\vec{r}) = 0 \tag{2.3}$$

$$k_i \frac{\partial T_j}{\partial n_i} + h_i T_j = \delta_{ij} f_i \tag{2.4}$$

Now each of the problems contains only one nonhomogeneous boundary condition. By superposition the solution is obtained to all of the sections as shown by equation (2.5).

$$T(\vec{r}) = \sum_{j=1}^{s} T_j(\vec{r}) \tag{2.5}$$

2.2.2. Application to Spacerless 3D Package Configuration

A spacerless 3D package primarily consists of two or more dice stacked on top of each other. Most common 3D packages use spacers between dice to create space for interconnects, but with a spacerless 3D package the number of components is reduced and takes a configuration in figure 2.2. Figure 2.2 shows a two layer stacked die architecture with same sized die stacked on top pf each other. This model is used to derive a steady state solution by Haji-Sheikh. [1] One nonhomogeneous boundary condition is applied to the stack and the separation of variable method is used to solve the temperature solution.

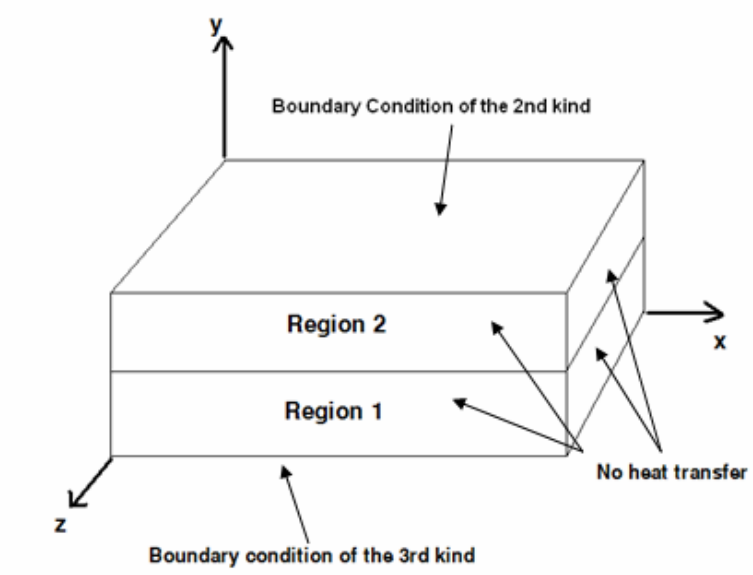

Figure 2.2: Schematic of Two Layer Package [1]

CHAPTER 3

OBJECTIVES AND APPROACH

The objective of this study is to extend a steady state solution to a spacerless 3D package with more than two layers. In doing so isotropic and orthotropic material properties, contact resistance, and non uniform power conditions will be considered.

3.1 Previous Work

Previous work (Haji-Sheikh et al) [1] has been done to develop steady-State heat conduction model in a two-layer body. Haji-Sheik's work provided solutions varying boundary conditions along with input power variations. It also incorporated the ability to apply a non-uniform power distribution. In that study a two layered spacerless 3D package was considered.

3.1.1. Methodology

Using the same method detailed by Haji-Sheikh [1] the temperature solutions for the two layered package is derived by using the diffusion equation. For the first layer and second layer the diffusion equation is as follows.

$$k_{1x}\frac{\partial^2 T_1}{\partial x^2}+k_{1y}\frac{\partial^2 T_1}{\partial y^2}+k_{1z}\frac{\partial^2 T_1}{\partial z^2}=0 \tag{3.1}$$

$$k_{2x}\frac{\partial^2 T_2}{\partial x^2}+k_{2y}\frac{\partial^2 T_2}{\partial y^2}+k_{2z}\frac{\partial^2 T_2}{\partial z^2}=0 \tag{3.2}$$

For a given region the temperature solution is represented by the following equation where X_j, Y_j, Z_j are eigenfunctions in the x, y and z directions respectively for each layer,

$$T_j(x,y,z,t)=X_j(x)Y_j(y)Z_j(z) \tag{3.3}$$

For region 1 the temperature solution is given by,

$$T_1(x,y,z,t)=X_1(x)Y_1(y)Z_1(z) \tag{3.4}$$

To obtain a similar solution for subsequent layers substitute X_j, Y_j, Z_j Eigen values for each layer in the x, y, z directions respectively. Applying separation of variables leads to the following equations,

$$k_{1x}\frac{X''}{X_1}+k_{1y}\frac{Y''}{Y_1}+k_{1z}\frac{Z''}{Z_1}=0 \tag{3.5}$$

$$k_{2x}\frac{X''}{X_2}+k_{2y}\frac{Y''}{Y_2}+k_{2z}\frac{Z''}{Z_2}=0 \tag{3.6}$$

Both the x-direction and z-direction have a homogeneous boundary condition and the physical dimensions are fixed, solutions for the eigenfunctions in those directions for each layer do not changed by layer and are given by equation (3.7) for the x direction and (9) for the z direction. β and ν are the eigenvalues for the given homogeneous boundary condition.

$$X_1=X_2=X_j=E\cos(\beta x)+F\sin(\beta x) \tag{3.7}$$

$$Z_1=Z_2=Z_j=G\cos(\nu x)+H\sin(\nu x) \tag{3.8}$$

Applying the corresponding homogeneous boundary conditions lead to the eigenfunctions β and ν in the x and z directions respectively. Substituting (3.7) and (3.8) to the diffusion equation gives the following result.

$$-k_{1x}\beta^2 + k_{1y}\frac{Y_1''}{Y_1} - k_{1z}\nu^2 = 0 \tag{3.9}$$

$$-k_{2x}\beta^2 + k_{2y}\frac{Y_2''}{Y_2} - k_{2z}\nu^2 = 0 \tag{3.10}$$

A generalized form of equations () with j denoting the corresponding layer is as follows.

$$-k_{ix}\beta^2 + k_{iy}\frac{Y_i''}{Y_i} - k_{iz}\nu^2 = 0 \tag{3.11}$$

The eigenvalue for the y-direction is given by γ_j, where the subscript j denotes the corresponding layer to which the eigenvalue applies. The eigenvalue for the y-direction is a function of the eigenvalues in the x and z directions and is obtained using the equation given below.

$$\gamma_j = \frac{k_{jx}}{k_{jy}}\beta^2 + \frac{k_{jz}}{k_{jy}}\nu^2 \tag{3.12}$$

Once the eigenvalues in the y-direction are known the eigenfunction in the y-directions can be represented by equation (3.13). Once the eigenvalues are known in the x, y, and z directions for the first layer, all of the corresponding eigenvalues and eigenfunctions in the y-direction can be found.

$Y_j = A_j \cosh(\gamma_j y) + B_j \sinh(\gamma_j y)$ (3.13)

The eigencoefficients A_j and B_j ican be found by applying the boundary conditions. For a boundary condition of the third kind on the bottom surface, A1=1 and B1=h/(kiy*γ_1).

3.1.2 Constraints and Boundary Conditions

The temperature solution can be found for the two layers once the eigenvalues β and ν are determined for the corresponding boundary conditions. The following boundary conditions are applied to the 3D package to resemble a functional package.

We will only to consider the temperature solution for the non homogeneous condition over the y=c surface where c is the total height of the package. Equation (3.14) gives the overall height.

$$c = \sum_{j=1}^{N} b_j \tag{3.14}$$

A boundary condition of the second kind with no heat transfer is applied to x=0, x=a, z=0, z=d surfaces of the package. All the heat is simulated to move to the top of the package without dissipating through the sides of the package.

Since the sides of the package are taken to be insulated and have no heat transfer on all side surfaces, the following boundary condition is applied over the corresponding surfaces,

$$\left.\frac{\partial T}{\partial x}\right|_{x=0,a} = 0 \tag{3.15}$$

$$\left.\frac{\partial T}{\partial z}\right|_{z=0,d} = 0 \tag{3.16}$$

The application of the boundary conditions result in the following simplified eigenfunctions in the x and z directions. β and ν represent the eigenvalues in the x and y directions respectively. Since a boundary condition on the x and z surfaces is taken to be adiabatic, the eigenfunctions are unchanged for each layer.

$$X_1 = X_2 = X_j = E\cos(\beta x) \tag{3.17}$$

$$Z_1 = Z_2 = Z_j = G\cos(\nu x) \tag{3.18}$$

Knowing the eigencoefficients and the eigenvalues the temperature solution can be calculated. The temperature solution is calculated using the following equations. A_{mn} is the orthoganility condition (A_{mn}) given by equation (3.20), where q_0 is the heat flux at the top surface in watts/ cm^2 and $N_{x,m}, N_{z,n}$ are the norms for the x and z directions.

$$T_j(x,y,z) = \sum_{m=0}^{\infty}\sum_{n=0}^{\infty} A_{mn} X_m(x) Y_{j,mn}(y) Z_n(z) \tag{3.19}$$

$$A_{mn} = \frac{-1}{k_{Ny} N_x N_z \gamma_N Y_N'(c)} \times \int_{z'}^{d}\int_{x'}^{a} q_0(x',z') X_m Z_n dx' dz' \tag{3.20}$$

For layer 1 the temperature solution is given by equation (3.21).

$$T_1(x,y,z) = \sum_{m=0}^{\infty}\sum_{n=0}^{\infty} A_{mn} X_m(x) Y_{1,mn}(y) Z_n(z) \tag{3.21}$$

3.2 Objectives of Extended Analytical solution for Spacerless Package

The primary objective is to calculate the temperature distribution in a spacerless 3D package with 3 or more layers. Knowing the eigenfunctions for the first layer we can derive the eigenfunctions in the y-direction once the eigencoefficients for all layers are known. A recursive relation is derived for the eigencoefficients so that a eigenfunctions can be obtained for N layers. Each eigencoefficient will be a function of the eigencoefficients of the previous layer which is know. The derivation ad solving process is as follows.

CHAPTER 4

ANALYTICAL MODELING OF 3D PACKAGE

Taking the model developed by Haji-Sheikh the number of layers is increased. The boundary conditions for the top and bottom layers are prescribed, the layers between will be constrained by the compatibility conditions between the layers. Using the compatibility conditions the Eigen coefficients are calculated in a recursive format. A description of the derivation process to obtain a recursive relation between layers follows.

4.1 Extension of Analytical Model

A package of 3 or more layers is used to derive the recursive relation between layers. The generalized eigenfunction in the y-direction is derived so that the eigencoefficients A_j and B_j are obtained for the first layer, the sobriquet eigencoefficients in layers two through N can be obtained for the eigenfunction. The thickness of each layer is independent of the other layers and is denoted by d_j for each corresponding layer. For simplification purposes, d is taken to be the same in all calculations.

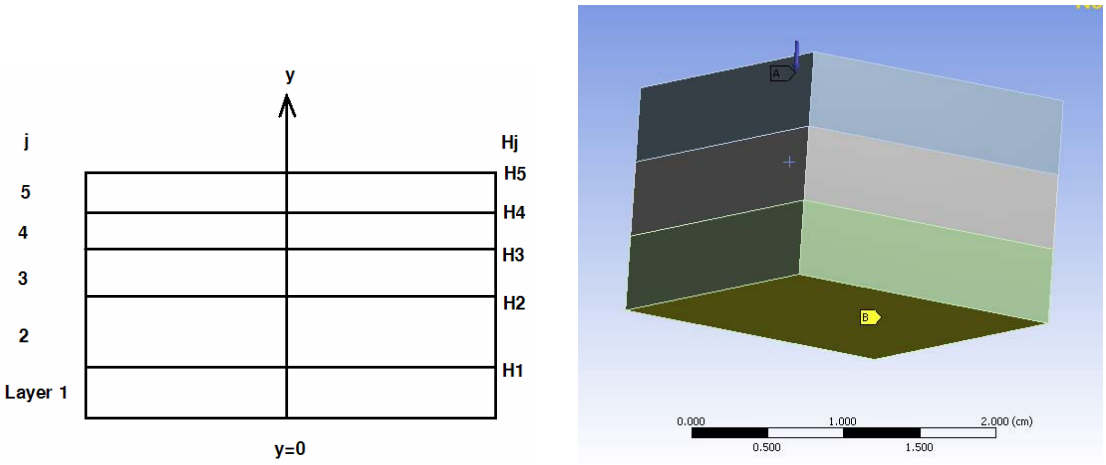

Figure 4.1: Five layer stacked package extension, and three-layer package model.

The contact resistance is taken to be R_j, where R_j is the resistance between layer j and j+1. The eigenvalues in the x and z direction are the same as shown in the two layered stack. [1] The separation of variables leads to the following equation for the eigenvalues in the y-direction. The generalized form of the eigenfunction in the y-direction is given in equation (4.1).

$$Y_j = A_j \cosh(\gamma_j y) + B_j \sinh(\gamma_j y) \tag{4.1}$$

Where γ_j is the spatial eigenvalues for layer j. The thermal conductivity for layer j is given by k_j and may vary with each layer. A_j and B_j are the coefficients for the eigenvalues. A_1 and B_1 can be equal to 1 at y=0. For the second layer the eigenvalues are given by,

$$Y_{j+1} = A_{j+1} \cosh(\gamma_{j+1} y) + B_{j+1} \sinh(\gamma_{j+1} y) \tag{4.2}$$

4.1.1 Recursive Relations of Eigen Coefficients

The eigenfunction in the y-direction takes two forms. One for γ Equal to Zero for γ Not Equal to Zero. Both instances are derailed as follows.

4.1.1.1 Eigen Coefficients for γ Not Equal to Zero

To compute the eigenvalues for consecutive layers the coefficients A_j and B_j are calculated for 1 < j < N. Using the contact conditions between layers yields the following equations,

$$\mathrm{k_j} = \left.\frac{\mathrm{dY_j}}{\mathrm{dy}}\right|_{y=H_j} = C_j (Y_{j+1} - Y_j)\Big|_{y=H_j} \qquad \text{for } \mathrm{j < N} \tag{4.3}$$

$$\mathrm{k_j} = \left.\frac{\mathrm{dY_j}}{\mathrm{dy}}\right|_{y=H_j} = k_{j+1}\left.\frac{dY_{j+1}}{dy}\right|_{y=H_j} \text{ for } \mathrm{j < N} \tag{4.4}$$

Solving equations (13) through (16) gives the following simultaneous relations,

$$\psi_{1,j+1} = A_{j+1}Cosh(\gamma_{j+1}H_j) + B_{j+1}Sinh(\gamma_{j+1}H_j) \tag{4.5}$$

$$\psi_{1,j+1} = A_{j+1}Cosh(\gamma_{j+1}H_j) + B_{j+1}Sinh(\gamma_{j+1}H_j) \tag{4.6}$$

Where,

$$\psi_{1,j+1} = [A_j Cosh(\gamma_{j+1}H_j) + B_j Sinh(\gamma_{j+1}H_j)] + \frac{\gamma_j k_j}{C_j}[A_j Sinh(\gamma_j H_j) + B_j osh(\gamma_j H_j)] \tag{4.7}$$

$$\psi_{2,j+1} = \frac{\gamma_j k_j}{k_{j+1}\gamma_{j+1}}[A_j Sinh(\gamma_j H_j) + B_j osh(\gamma_j H_j)] \tag{4.8}$$

Solving equations (19) and (20) for coefficients A_{j+1}, B_{j+1} gives,

$$A_{j+1} = \psi_{1,j+1}\ \mathrm{Cosh}(\gamma_{j+1}H_j) - \psi_{2,j+1}\ \mathrm{Sinh}(\gamma_{j+1}H_j) \tag{4.9}$$

$$B_{j+1} = -\psi_{1,j+1}\ \mathrm{Sinh}(\gamma_{j+1}H_j) + \psi_{2,j+1}\ \mathrm{Cosh}(\gamma_{j+1}H_j) \tag{23}$$

Using the results to substitute back to equations (13) and (14) gives,

$$Y_{j+1} = [\psi_{1,j+1}Cosh(\gamma_{j+1}H_j) - \psi_{2,j+1}Sinh(\gamma_{j+1}H_j)]Cosh(\gamma_{j+1}y) + [-\psi_{1,j+1}Sinh(\gamma_{j+1}H_j) + \psi_{2,j+1}Cosh(\gamma_{j+1}H_j)]Sinh(\gamma_{j+1}y) \tag{4.10}$$

$$Y_{j+1} = A_{j+1}\ \mathrm{Cosh}[\gamma_{j+1}(y - H_j)] - B_{j+1}\ \mathrm{Sinh}[\gamma_{j+1}(y - H_j)] \tag{4.11}$$

Defining $\bar{y}_{j+1} = (y - H_j)$ the eigenfunction takes the form,

$$Y_{j+1} = \psi_{1,j+1}\ \mathrm{Cosh}(\gamma_{j+1}\bar{y}_{j+1}) - \psi_{2,j+1}\ \mathrm{Sinh}(\gamma_{j+1}\bar{y}_{j+1}) \tag{4.12}$$

This equation is in the same form as equation (10) and can be written as,

$$Y_{j+1} = A_{j+1}\ \mathrm{Cosh}(\gamma_{j+1}\bar{y}_{j+1}) - B_{j+1}\ \mathrm{Sinh}(\gamma_{j+1}\bar{y}_{j+1}) \tag{4.13}$$

Then Y_j can be written as,

$$Y_j = A_j\ \mathrm{Cosh}(\gamma_j\bar{y}_j) - B_j\ \mathrm{Sinh}(\gamma_j\bar{y}_j) \tag{4.14}$$

From these relations we can conclude that $\psi_{1,j}$ and $\psi_{2,j}$ have the same function as A_j and B_j the coefficients in the eigenfunction. A recursive relation is can be formed by substitution the two parameters.

$$A_{j+1} = [A_jCosh(\gamma_{j+1}H_j) + B_jSinh(\gamma_{j+1}H_j)] + \frac{\gamma_j k_j}{C_j}[A_jSinh(\gamma_jH_j) + B_josh(\gamma_jH_j)] \tag{4.15}$$

$$B_{j+1} = \frac{\gamma_j k_j}{k_{j+1}\gamma_{j+1}}[A_j Sinh(\gamma_j H_j) + B_j Cosh(\gamma_j H_j)] \tag{4.16}$$

Knowing the eigenfunction and its coefficient for layer 1 can give the eigenfunction and the eigencoefficients of layer 2 and subsequent layers to follow.

4.1.1.2 Eigen Coefficients for γ Equal to Zero

For the condition when γ= 0 the differential equation in the y-direction is given by equation (14.7).

$$\frac{Y_1''}{Y_1} = 0 \tag{4.17}$$

The solution to equation (14.7) is given below in equation (14.8). The coefficients E_j and F_j can be determined by applying the corresponding boundary conditions. The subscript j denotes the corresponding layer to which the coefficients belong. Applying the boundary conditions of convection on the bottom surface and a prescribed heat flux, a recursive relation is derived for E_j and F_j. After obtaining the solution for E_j and F_j the solution for the eigenfunction in the y-direction can be determined using equation (4.18)

$$Y_j = E_j + F_j y \tag{4.18}$$

$$E_{j+1} = E_j + F_j\left(\frac{k_j}{C_j} + d_j - \frac{k_j}{k_{j+1}} d_j\right) \tag{4.19}$$

$$F_{j+1} = \frac{k_j}{k_{j+1}} F_j \tag{4.20}$$

4.2 Dimensions and Material Properties

A 3D package consisting of 3 layers is chosen to apply the derived solution. The dimensions and material properties for are given in table 4.1below. The material properties are taken to be isotropic. The analytical solution is derived for orthotropic material properties. The subscript denoting the direction of the property is removes as isotropic properties are assigned.

Table 4.2: Dimensions and Material Properties of 3-Layer Package

Dimension	Value
Length, Width (a, d)	2 cm
Die Thickness (b_1, b_2, b_3)	0.5 cm
Total Package Height (c)	1.5 cm
Thermal Conductivity in layer 1,2 and 3 k_1, k_2, k_3	0.3 W/cm-K
Heat Flux Across Top Surface (q_0)	1.0 W/cm^2
Ambient Temperature (T_∞)	298 ^0K

CHAPTER 5

RESULTS AND DISCUSSION

Three types of nonhomogeneous boundary condition are chosen to be evaluated by the derived analytical model. Hot spot temperatures for all three layers are calculated for each condition.

1. Uniform heat flux distribution across the surface.

2. Heated regions, where $a_1/a = d_1/d = 0.1, 0.125, 0.25, 0.5, 0.75, 1.0$.

3. Heated regions, where $a_1/a = 0.25, 0.5, 0.75, 1.0$, and $d_1/d = 1.0$.

5.1 Uniform Heat Flux

Two instances are considered with a uniform hear flux of q_0 being applied on the top surface of the package. Contact resistance (C_j) is taken to be zero for perfect contact. The instances for perfect contact and a contact resistance of 0.1 cm^2-^{0}C/watt is considered.

5.1.1 Uniform Heat Flux with Perfect Contact

First we obtain the solution for the condition with perfect contact. The temperature solution in each layer is obtained separately. Using the contact conditions, if the contact resistance is set to be zero for perfect contact between layers there should be no discontinuity in the temperatures between each layer. Table 5.1 and Figure 5.1 illustrate the resulting temperature.

Table 5.1: Temperature Solution for Uniform Heat Flux with Perfect Contact.

Package Height (cm)	Temperature Layer 1 (C)	Temperature Layer 2 (C)	Temperature Layer 3 (C)
0	33.333		
0.1	34.666		
0.2	36.000		
0.3	37.333		
0.4	38.667		
0.5	40.000	40.000	
0.6		41.333	
0.7		42.667	
0.8		44.000	
0.9		45.333	
1		46.667	46.667
1.1			48.000
1.2			49.333
1.3			50.667
1.4			52.000
1.5			53.333

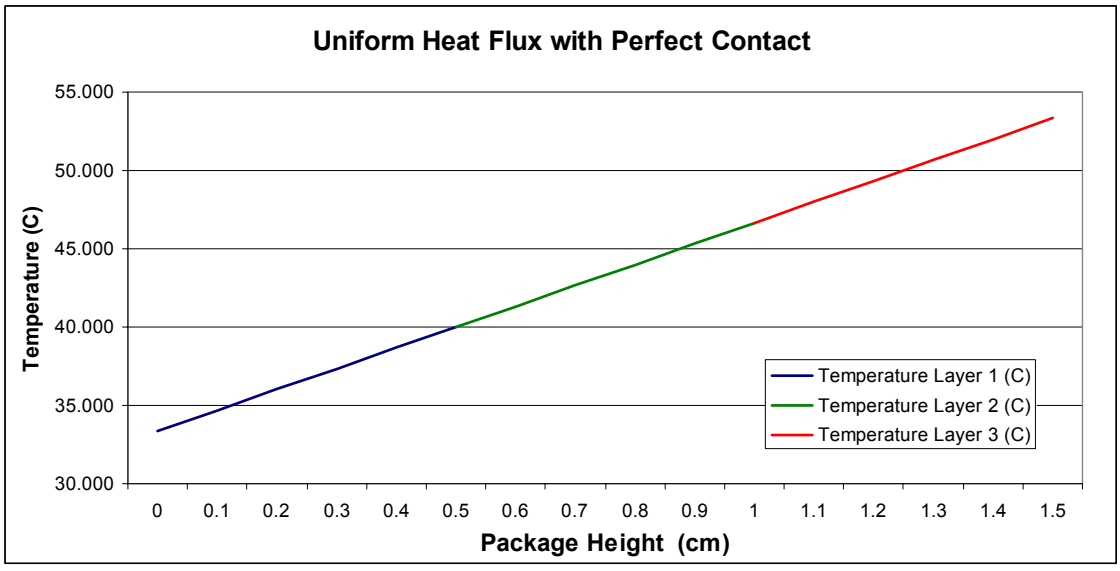

Figure 5.1: Temperature Solution for Uniform Heat Flux with Perfect Contact.

5.1.2 Uniform Heat Flux with Contact Resistance

A contact resistance of C=0.1 (cm^2-^{0}C/watt) is applied between layers

Table 5.2: Temperature for Uniform Heat Flux with Contact Resistance.

Height (cm)	Temperature Layer 1 (C)	Temperature Layer 2 (C)	Temperature Layer 3 (C)
0	33.333		
0.1	34.666		
0.2	36.000		
0.3	37.333		
0.4	38.667		
0.5	40.000	40.400	
0.6		41.733	
0.7		43.067	
0.8		44.400	
0.9		45.733	
1		47.067	47.467
1.1			48.800
1.2			50.133
1.3			51.467
1.4			52.800
1.5			54.133

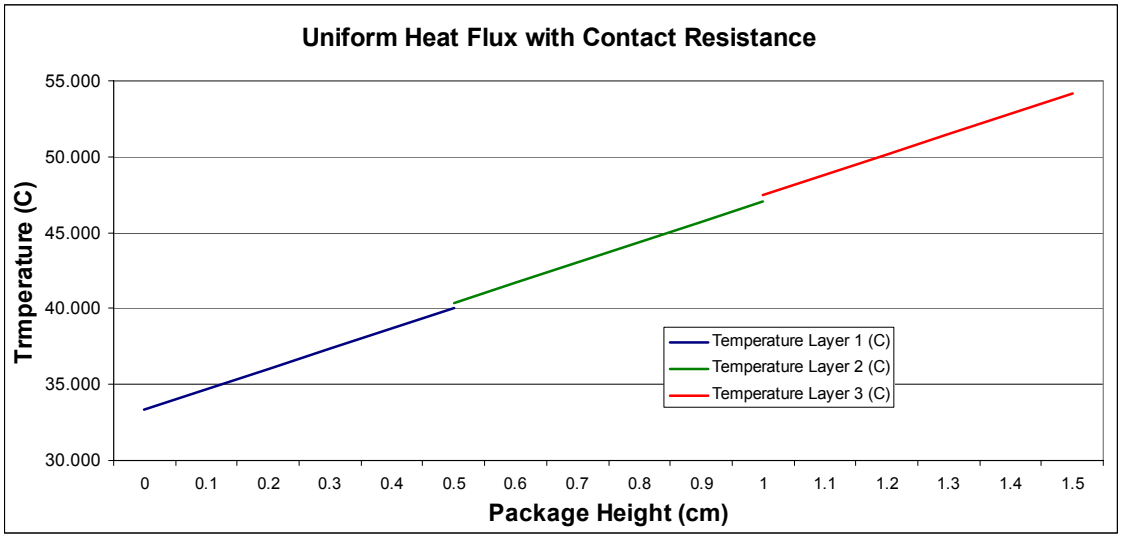

Figure 5.2: Temperature for Uniform Heat Flux with Contact Resistance. C=0.1 cm^2-K/watt

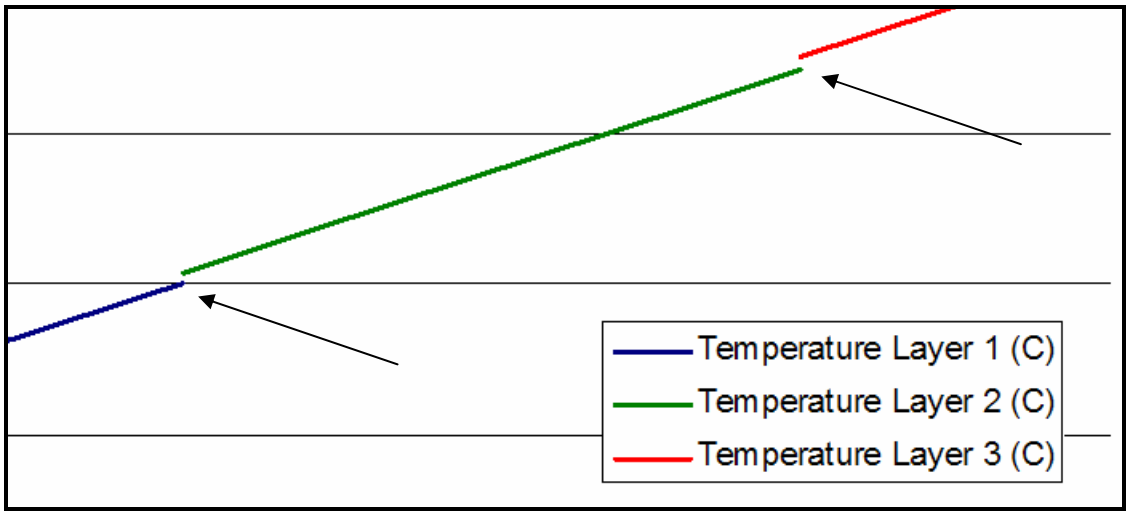

Figure 5.3: Discontinuity in Temperature Between layers.

5.2 Non Uniform Heat Flux

5.2.1 Non Uniform Heat Flux with Corner Heated Regions

The first non uniform heated region considered is a square region set at the origin. The length and the width of the heated region is varied from, 10% of the package length and width to 75% of the package length and width. The 100% heated instance will be non uniform hear flux. Figure 5.3 illustrates the heated region which is considered to be a non uniform heat distribution.

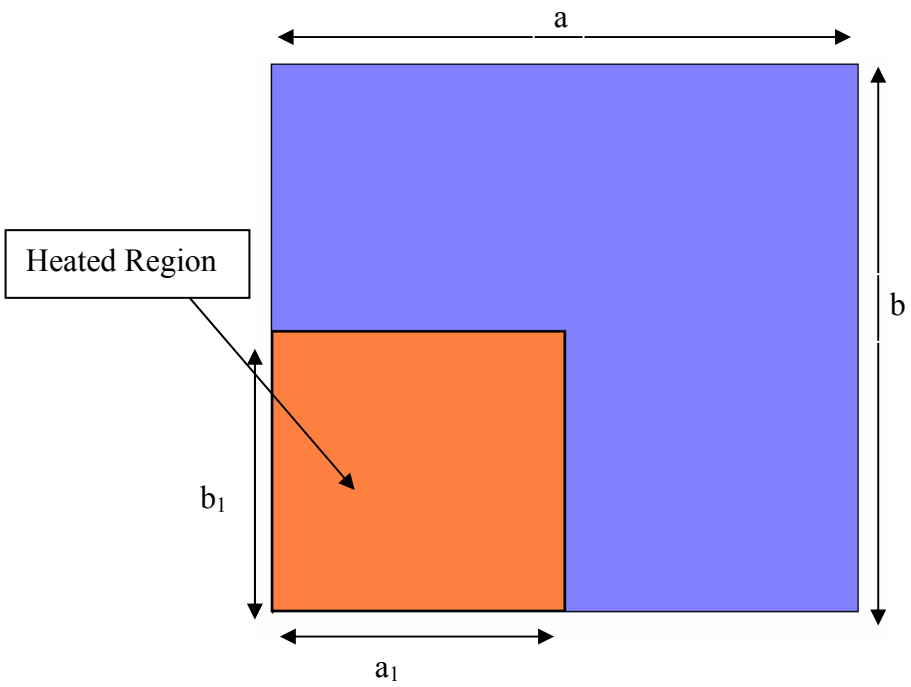

Figure 5.4: Square Corner Heated Region

The results to the heated religions are given in tables 5.3 to 5.7 below. The hot spot temperatures are taken for each later. Contour plots and 3-dimensional plots are also listed.

5.2.1.1 Heated Region a1/a =d1/d=0.1

Table 5.3: Heated Region a1/a =d1/d=0.1

Layer	Hot Spot Temperature(C)
1	0.402
2	0.474
3	0.570

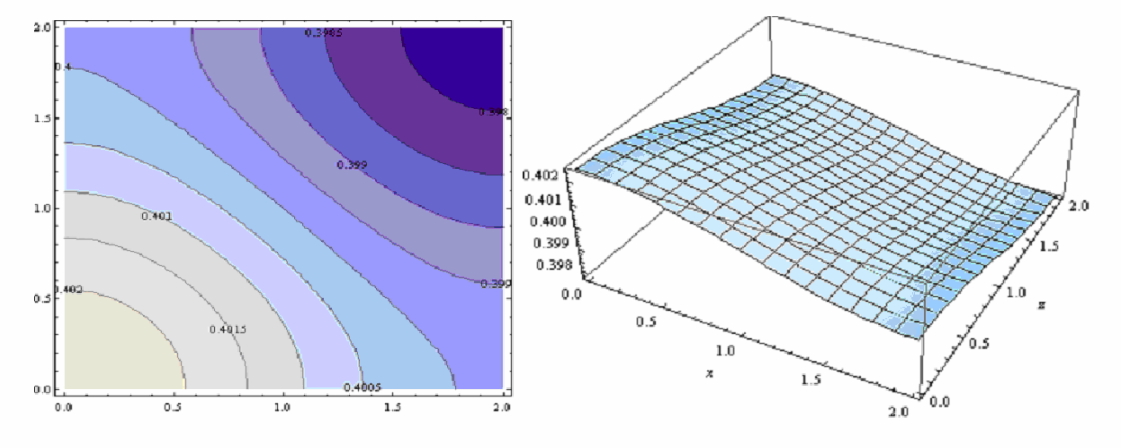

Figure 5.5: Layer 1 Hot Spot Temperature for Heated Region a1/a =d1/d=0.1

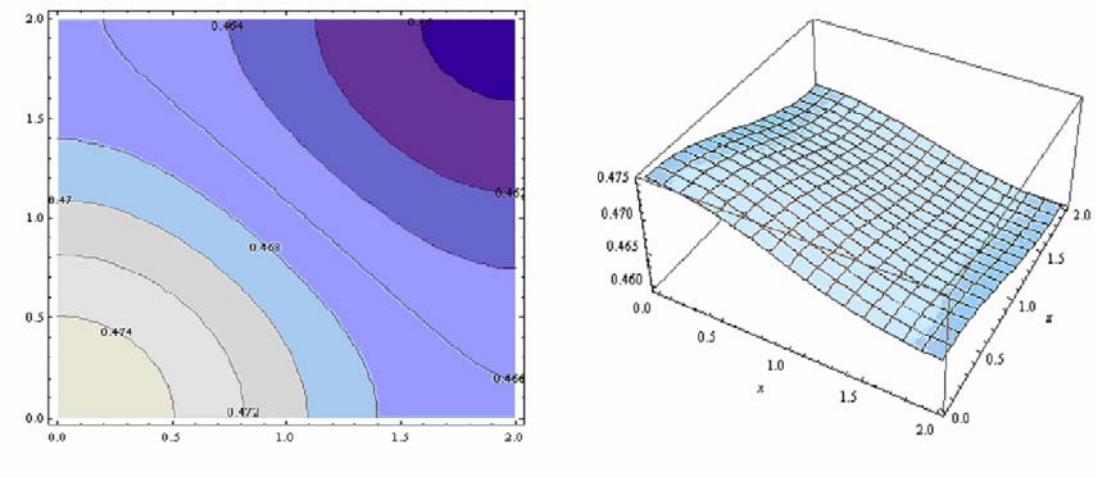

Figure 5.6: Layer 2 Hot Spot Temperature for Heated Region a1/a =d1/d=0.1

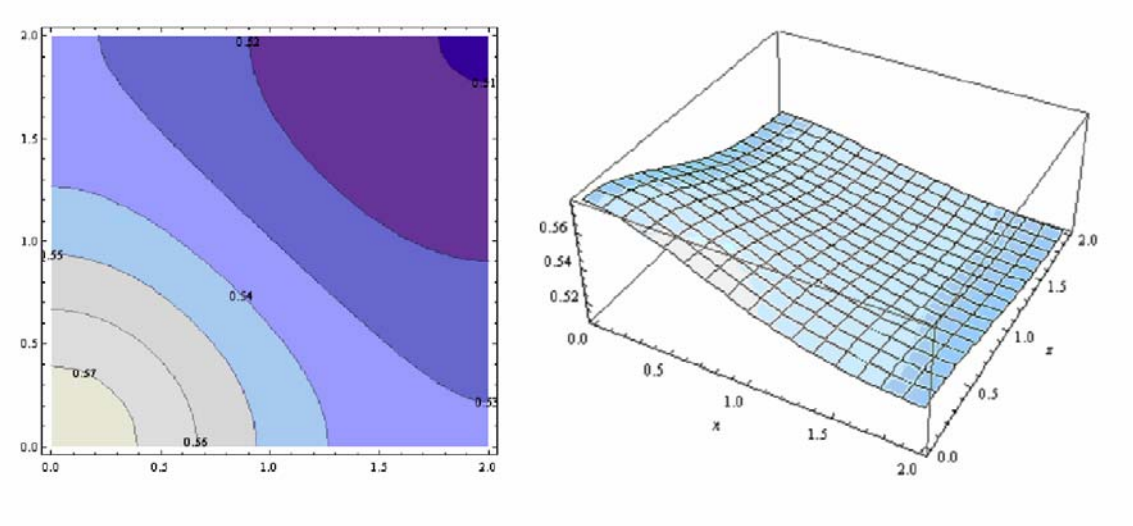

Figure 5.7: Layer 3 Hot Spot Temperature for Heated Region a1/a =d1/d=0.1

5.2.1.2 Heated Region a1/a =d1/d=0.125

Table 5.4: Heated Region a1/a =d1/d=0.125

Layer	Hot Spot Temperature(C)
1	0.682
2	0.740
3	0.900

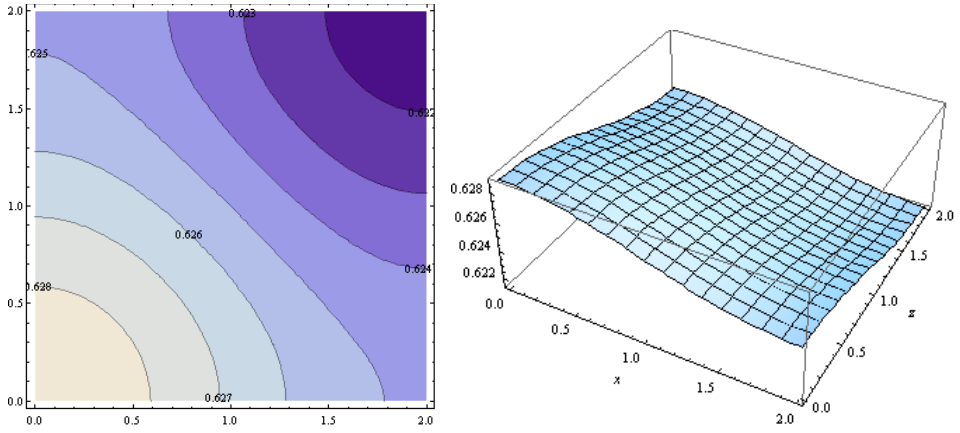

Figure 5.8: Layer 1 Hot Spot Temperature for Heated Region a1/a =d1/d=0.125

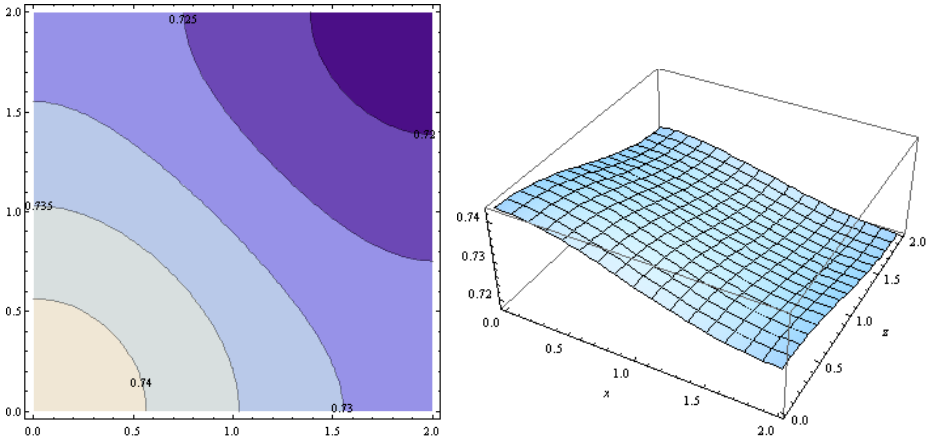

Figure 5.9: Layer 2 Hot Spot Temperature for Heated Region a1/a =d1/d=0.125

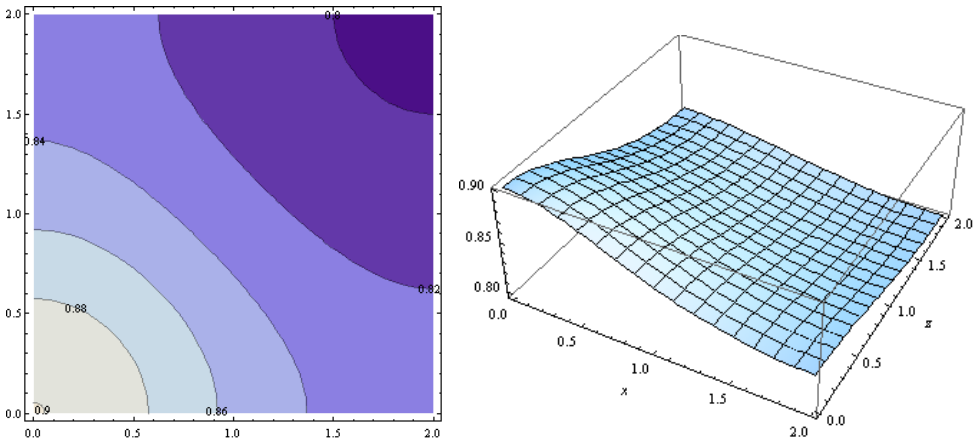

Figure 5.10: Layer 3 Hot Spot Temperature for Heated Region a1/a =d1/d=0.125

5.2.1.3 Heated Region a1/a =d1/d=0.25

Table 5.5: Heated Region a1/a =d1/d=0.25

Layer	Hot Spot Temperature(C)
1	2.510
2	2.960
3	3.550

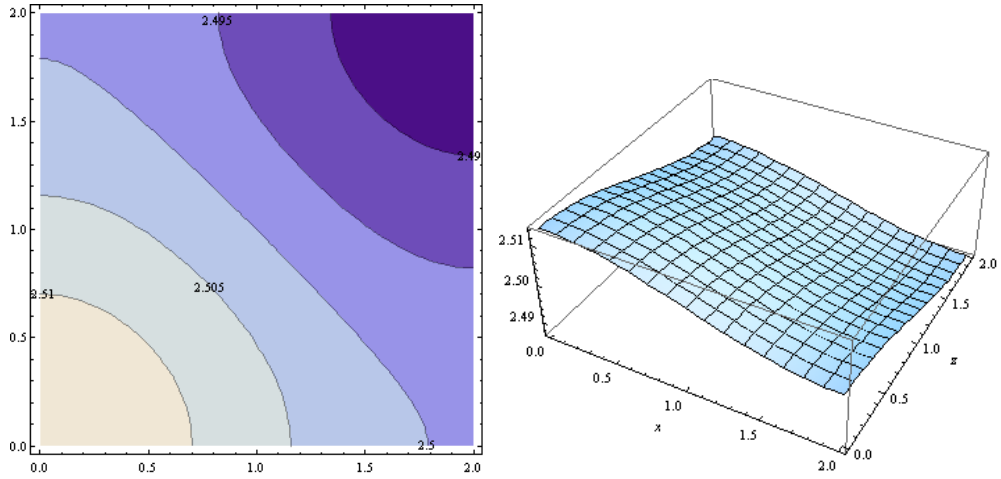

Figure 5.11: Layer 1 Hot Spot Temperature for Heated Region a1/a =d1/d=0.25

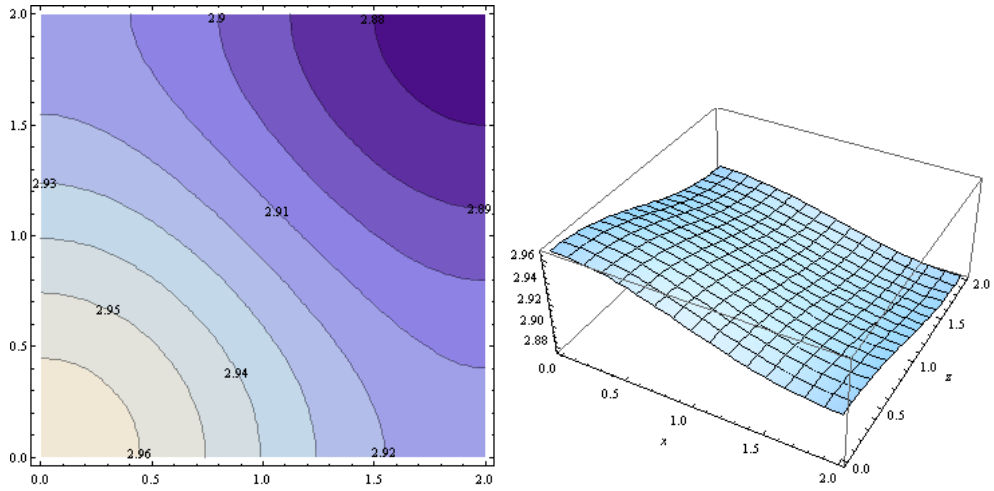

Figure 5.12: Layer 2 Hot Spot Temperature for Heated Region a1/a =d1/d=0.25

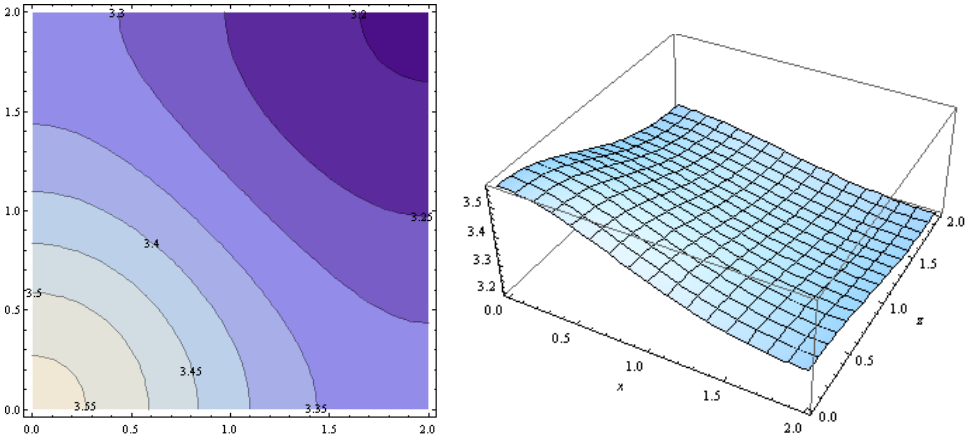

Figure 5.13: Layer 3 Hot Spot Temperature for Heated Region a1/a =d1/d=0.25

5.2.1.4 Heated Region a1/a =d1/d=0.5

Table 5.6: Heated Region a1/a =d1/d=0.5

Layer	Hot Spot Temperature(C)
1	10.030
2	11.800
3	13.800

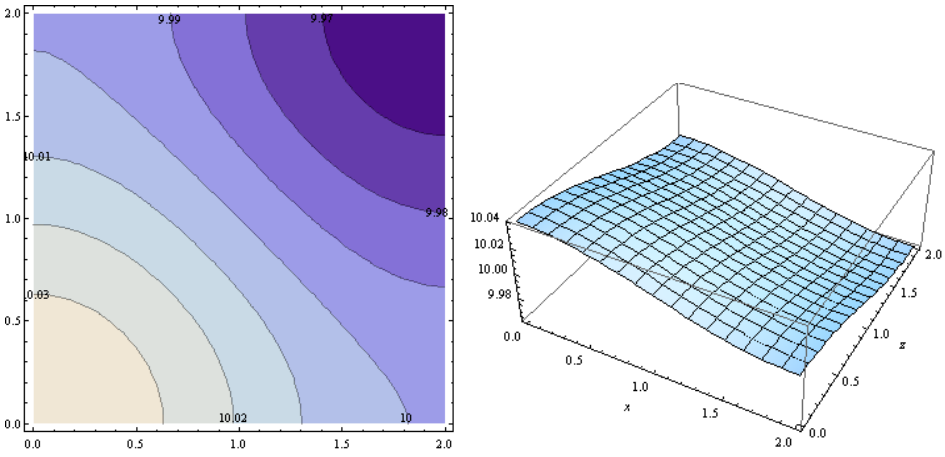

Figure 5.14: Layer 1 Hot Spot Temperature for Heated Region a1/a =d1/d=0.5

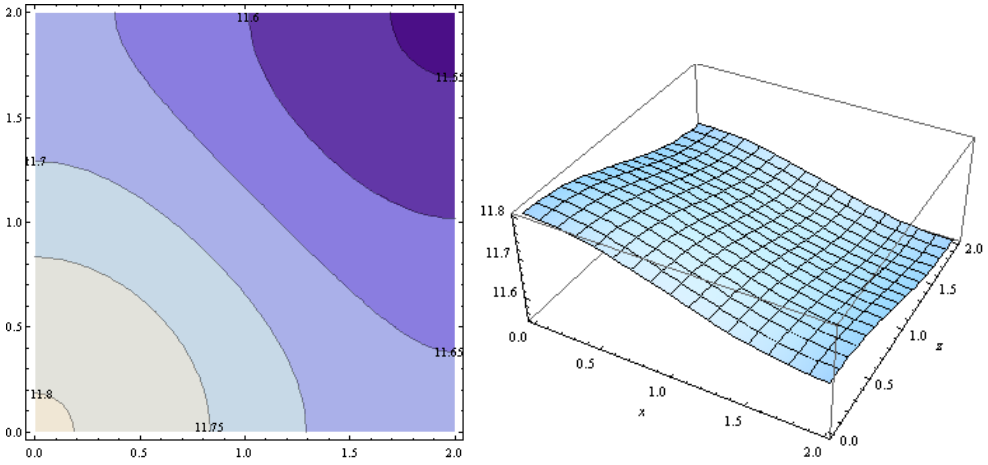

Figure 5.15: Layer 2 Hot Spot Temperature for Heated Region a1/a =d1/d=0.5

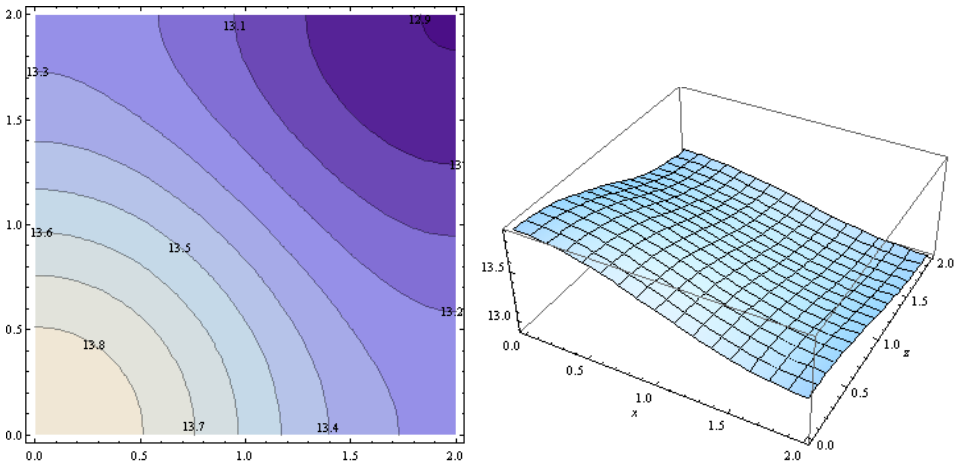

Figure 5.16: Layer 3 Hot Spot Temperature for Heated Region a1/a =d1/d=0.5

5.2.1.5 Heated Region a1/a =d1/d=0.75

Table 5.7: Heated Region a1/a =d1/d=0.75

Layer	Hot Spot Temperature(C)
1	22.540
2	26.350
3	30.400

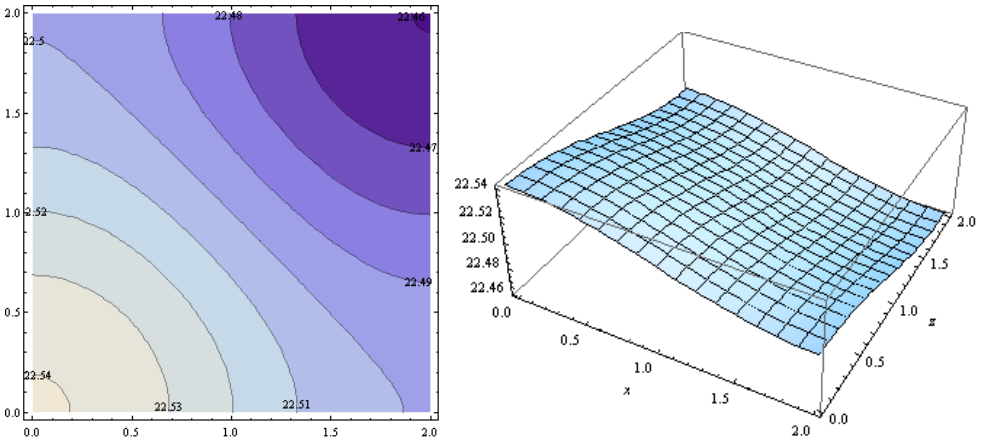

Figure 5.17: Layer 1 Hot Spot Temperature for Heated Region a1/a =d1/d=0.75

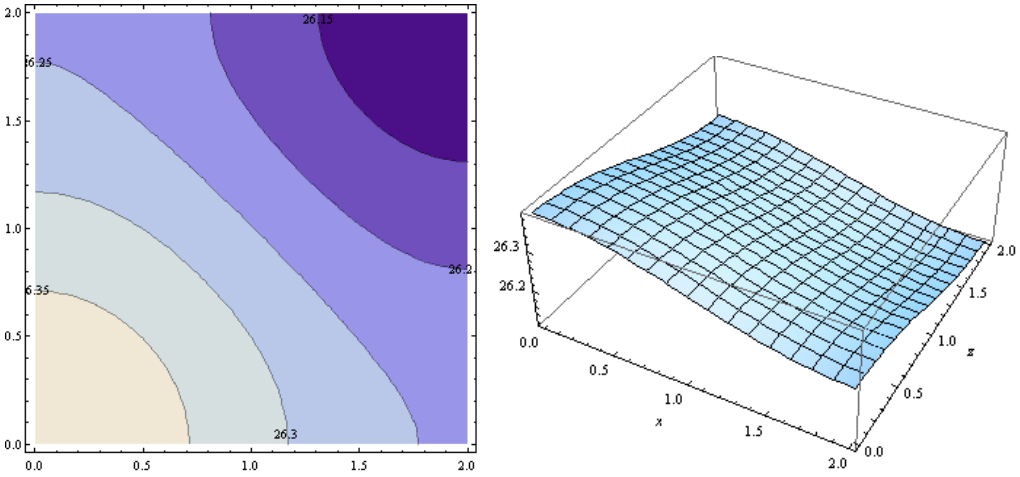

Figure 5.18: Layer 2 Hot Spot Temperature for Heated Region a1/a =d1/d=0.75

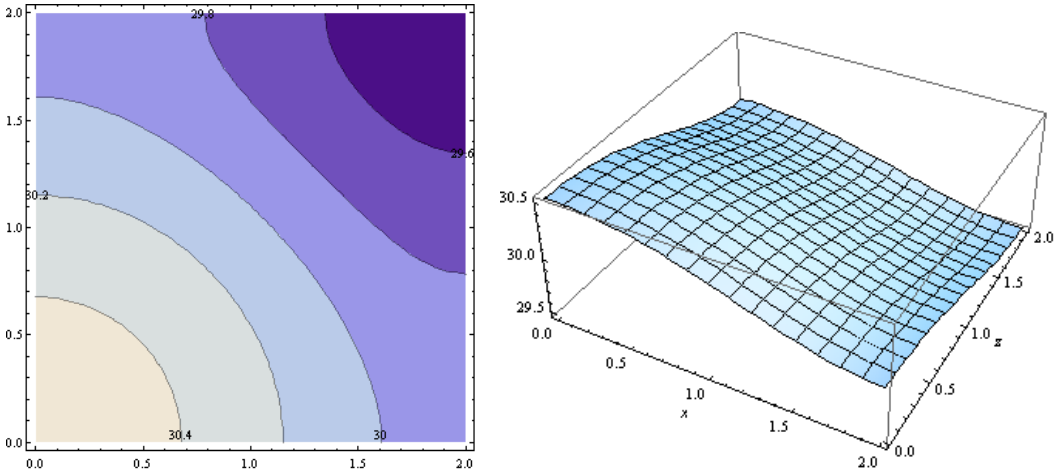

Figure 5.19: Layer 3 Hot Spot Temperature for Heated Region a1/a =d1/d=0.75

For comparison the dimensionless hot spot temperature is calculated for each heated condition above using equation (5.1) in the three layer stack. Table 5.8 gives the results

$$T_D = k_1(T - T_\infty)/(aq_0) \tag{5.1}$$

Table 5.8: Dimensionless Hot Spot Temperatures

Heated Region (a1/a =d1/d)	**Dimensionless Hot Spot Temperature** (T_D)
0.100	0.855
0.125	0.135
0.250	0.533
0.500	2.070
0.750	4.560
1.000	7.999

5.2.2 Non Uniform Heat Flux with Corner Heated Regions

The instance where one side of the package is heated is considered. The heated region is taken where d1/d=1.0 while a1/a =0.25, 0.5,0.75 and 1.0 is considered. This configuration heats one side if the package and increases the thickness of the heated region until the whole package is heated uniformly. Table 5.9 gives the corresponding results.

Table 5.9: Hot spot and dimensionless hot spot temperature for strip heated regions.

Heated Region a1/a with d1/d=1.0	Hot Spot Temperature ©	Dimensionless Hot Spot Temperature
0.250	13.600	2.040
0.500	27.000	4.050
0.750	40.020	6.003
1.000	50.333	7.999

The plots illustrating the results for hot spot temperature is given below. The highest temperature occurs on the layer 3. Only T_3 results are shown.

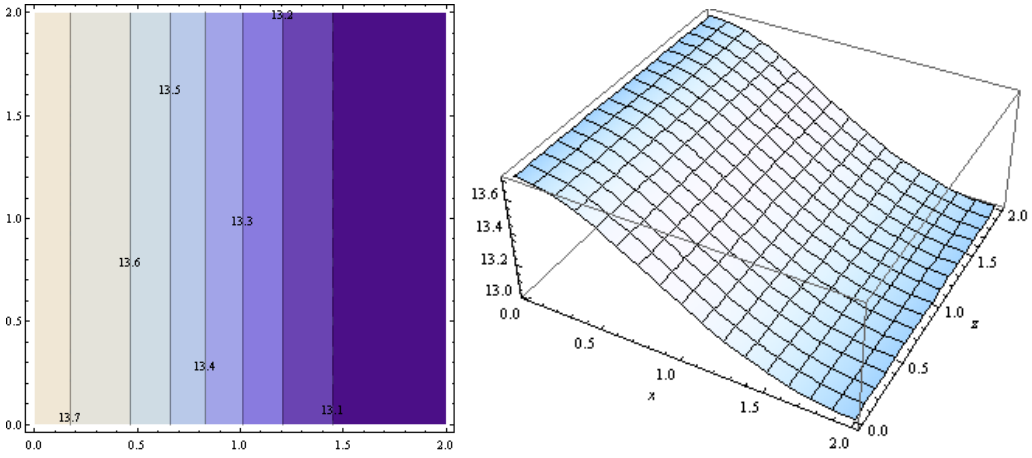

Figure 5.20: Maximum Temperature Distribution for a1/a = 0.25, d1/d=1.0

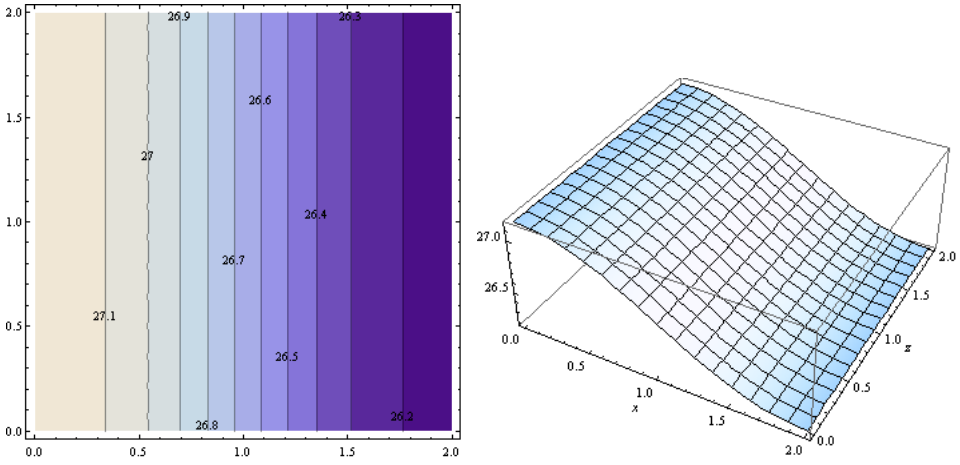

Figure 5.21: Maximum Temperature Distribution for a1/a = 0.5, d1/d=1.0

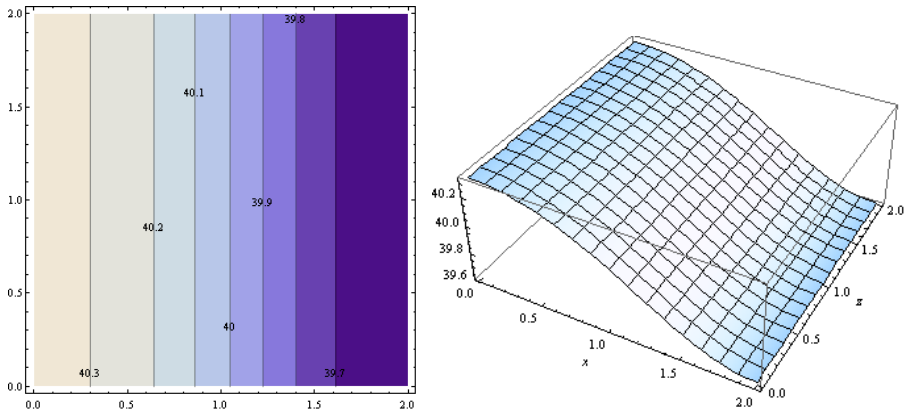

Figure 5.22: Maximum Temperature Distribution for a1/a = 0.75, d1/d=1.0

5.3 Conclusions

In this study the derivation of an analytical solution of a spacerless 3D package detailed by Hajji-Sheikh [1] has been extended to include an increase number of layers in a single stack. The solution is achieved by formulating a recursive relationship between adjoining layers. As detailed for the two layers stack the separation of variables

method is used to obtain an analytical solution to the 3-dimensional heat conduction problem. Mathematica is used to solve the derived analytical solution and several package configurations are used. Parameters such as orthotropic material properties, contact resistances between surfaces and non uniform heat distribution are accounted for within the solution. The solution reveals the non uniform heat distribution creates hot spots within the package. Further investigation with varying power, constraints and material properties are possible with this solution.

APPENDIX A

PROGRAM IN MATHEMATICA FOR UNIFORM HEAT FLUX IN SPACERLESS 3-LAER STACKED DIE PACKAGE

```
d=2;
a=2;
c=1.5;
b1=0.5;
b2=0.5;
b3=0.5;
k1x=0.3;
k1y=0.3;
k1z=0.3;
k2x=0.3;
k2y=0.3;
k2z=0.3;
k3x=0.3;
k3y=0.3;
k3z=0.3;
h=0.4;

C1=0;
C2=0;

A1=1;
B1=h/(k1y*γ1);
E1=1;
F1=h*E1;

H1=b1;
H2=b1+b2;
H3=b1+b2+b3;

β[m_]=m*π/a;
ν[n_]=n*π/d;

γ1=Sqrt[((k1x/k1y)*β[m]^2)+((k1z/k1y)*ν[n]^2)];
γ2=Sqrt[((k2x/k2y)*β[m]^2)+((k2z/k2y)*ν[n]^2)];
γ3=Sqrt[((k3x/k3y)*β[m]^2)+((k3z/k3y)*ν[n]^2)];

X[m_]:=Cos[β[m]*x]/;m>0
X[m_]:=1/;m==0
Z[n_]:=Cos[ν[n]*z]/;n>0
Z[n_]:=1/;n==0

nx[m_]:=a/;m≤0
nx[m_]:=a/2/;m>0
nz[n_]:=d/;n≤0
nz[n_]:=d/2/;n>0

A2=A1*Cosh[γ1*b1]+B1*Sinh[γ1*b1]+(γ1*k1y*C1)*A1*Sinh[γ1*b1]+(γ1*k1y*C1)*B1*Cosh[γ1*b
1];
B2=(k1y*γ1/k2y*γ2)*(A1*Sinh[γ1*b1]+B1*Cosh[γ1*b1]);
A3=A2*Cosh[γ2*b2]+B2*Sinh[γ2*b2]+(γ2*k2y*C2)*A2*Sinh[γ2*b2]+(γ2*k2y*C2)*B2*Cosh[γ2*b
2];
```

```
B3=(k1y*γ1/k3y*γ3)*(A2*Sinh[γ2*b2]+B2*Cosh[γ2*b2]);

E2=E1+F1 ((k1y*C1)+b1-((k1y/k2y)*b1));
F2= (k1y/k2y)*F1;
E3=E2+F2 ((k2y*C2)+b2-((k2y/k3y)*b2));
F3= (k2y/k3y)*F2;

Y1=If[m+n==0,E1+(F1*y),A1*Cosh[(γ1)*y]+B1*Sinh[(γ1)*y]];
Y2=If[m+n==0,E2+(F2*y),A2*Cosh[(γ2)*(y-H1)]+B2*Sinh[(γ2)*(y-H1)]];
Y3=If[m+n==0,E3+(F3*y),A3*Cosh[(γ3)*(y-H2)]+B3*Sinh[(γ3)*(y-H2)]];

q0=1;

Y3C=If[m+n==0,F3,γ3 (A3*Sinh[γ3*c]+B3*Cosh[γ3*c])];

T1[x_,y_,z_]=-1*Sum[X[m]*Z[n]*Y1*(1/(k3y*(a/2)*(d/2)))*(-
1/(Y3C))*Integrate[q0*X[m]*Z[n],{x,0,2},{z,0,2}],{m,0,10},{n,0,10}];

T2[x_,y_,z_]=-1*Sum[X[m]*Z[n]*Y2*(1/(k3y*(a/2)*(d/2)))*(-
1/(Y3C))*Integrate[q0*X[m]*Z[n],{x,0,2},{z,0,2}],{m,0,10},{n,0,10}];
T2[1,0.5,1]

T3[x_,y_,z_]=-1*Sum[X[m]*Z[n]*Y3*(1/(k3y*(a/2)*(d/2)))*(-
1/(Y3C))*Integrate[q0*X[m]*Z[n],{x,0,2},{z,0,2}],{m,0,10},{n,0,10}];
```

REFERENCES

[1] A. Haji-Sheikh, J.V. Beck, D. Agonafer. (2003). Steady-state heat conduction in multi-layer bodies, Journal of Heat and Mass Transfer, 46**,** pp 2363-2379.

[2] J.V. Beck, K. Cole, A. Haji-Sheikh, B. Litkouhi. (1992). Heat conduction using Green's functions, Hemisphere Publications Corp. Washington D.C.

[3] A. Haji-Sheikh, J.V. Beck. (2000). An efficient method of computing Eigenvalues in heat conduction, Number. Heat Transfer, B 38, pp 133-156.

[4] Cooling Zone: Web reference: www.coolingzone.com

[5] Roksana Akhter, (2004) "Optimal Thermal Management of Stacked Die Package: Design For stackibility" University of Texas, Arlington.

[6] Hossain, M. M., Yong-Je Lee, Roksana Akhter, Senol pekin, (2006). Reliability of Stack Packaging Varing the Die Stacking Architecture for Flash Memory Applications, Semi-Therm 22th

[7] Akhter, R., Sandur, B. P. D. Hossain, M.M, Kaisare, A., Lawrence. K. , Agonafer, D., Pekin, S., and Dishongh, T.," Thermal comparison of die stacking architectures for Flash Memory Applications" , IMECE 05.

[8] S. Borkar, "Design challenges of technology scaling," *IEEE Micro*, pages 23–29, Jul.–Aug. 1999.

[9] Larry Wu, Yu-Po Wang, S.C. Kee*, Bob Wallace*,**C.S** Hsiao, C.K Yeh, T.D. Her, and Randy Lo. (2000). Siliconware Precision Industries Co., Ltd.

[10] Chan, Y.S.; Lee, S.W.R.,(2006) Thermal Resistance Analysis of a Multi-Stack Flip Chip 3-D Package, . Electronics Manufacturing Technology Symposium, Twenty-Sixth IEEE/CPMT International. pp 102 – 107

[11] Wu, L., Yu-Po Wang, Kee, S.C., Wallace, B., Hsiao, C.S., Yeh, C.K., Her, T.D., Lo, R., (2000). Twenty-Sixth IEEE/CPMT International, pp 102 – 107.

[12] Y. K. Tsui and S. W. Ricky, "Design and Fabrication of a Flip-Chip-on-Chip 3D Packaging Structure with a Through-Silicon Via for Underfill Dispensing, (2005). Hong Kong University of Science.

[13] Akhter, R., Sandur, B.P.D., Hossain, M., Kaisare, A., Agonafer, D., Lawrence, K., Dishongh, T., (2005), Design for stackability of flash memory devices based on thermal optimization, Digital Avionics Systems Conference, DASC 2005. The 24th Volume 2.

[14] Özişik, N.M.,(1993), Heat Conduction, Second Edition, Wiley, New York.

BIOGRAPHICAL INFORMATION

Nuwan Rodrigo received a Bachelor of Science in Mechanical Engineering form the University of Texas Arlington in December 2003 and Master of Science in Mechanical Engineering form the University of Texas Arlington in August 2008.